Late Cretaceous bird from Madagascar reveals unique development of beaks

https://doi.org/10.1038/s41586-020-2945-x

Received: 30 April 2020

Accepted: 14 September 2020

Published online: 25 November 2020

Check for updates

Patrick M. O'Connor[1,2,3]✉, Alan H. Turner[4], Joseph R. Groenke[1], Ryan N. Felice[5], Raymond R. Rogers[3,6], David W. Krause[3,4] & Lydia J. Rahantarisoa[7]

Mesozoic birds display considerable diversity in size, flight adaptations and feather organization[1–4], but exhibit relatively conserved patterns of beak shape and development[5–7]. Although Neornithine (that is, crown group) birds also exhibit constraint on facial development[8,9], they have comparatively diverse beak morphologies associated with a range of feeding and behavioural ecologies, in contrast to Mesozoic birds. Here we describe a crow-sized stem bird, *Falcatakely forsterae* gen. et sp. nov., from the Late Cretaceous epoch of Madagascar that possesses a long and deep rostrum, an expression of beak morphology that was previously unknown among Mesozoic birds and is superficially similar to that of a variety of crown-group birds (for example, toucans). The rostrum of *Falcatakely* is composed of an expansive edentulous maxilla and a small tooth-bearing premaxilla. Morphometric analyses of individual bony elements and three-dimensional rostrum shape reveal the development of a neornithine-like facial anatomy despite the retention of a maxilla–premaxilla organization that is similar to that of nonavialan theropods. The patterning and increased height of the rostrum in *Falcatakely* reveals a degree of developmental lability and increased morphological disparity that was previously unknown in early branching avialans. Expression of this phenotype (and presumed ecology) in a stem bird underscores that consolidation to the neornithine-like, premaxilla-dominated rostrum was not an evolutionary prerequisite for beak enlargement.

Our understanding of the evolution of Mesozoic birds continues to improve, driven predominantly by discoveries from the Early Cretaceous epoch of China[1–3,6]. Although these specimens show considerable variation in body size, soft-tissue anatomy and inferred ecologies[2–4,10,11], the disparity in Mesozoic avialan cranial shape remains restricted to a relatively limited number of forms that are considered to be either generalists or substrate-probing specialists[5,6,12–15] and represent groups that are only distantly related to crown birds. The Late Cretaceous (about 100–66 million years ago) chapter of avialan evolution remains relatively incomplete owing to a paucity of new fossil discoveries (although see recent studies on birds such as *Ichthyornis*[16] and *Asteriornis*[17]). Thus, new fossils of Late Cretaceous birds are essential for refining hypotheses that relate to the morphological evolution and diversification of avialans.

The phylogenetic diversity of early branching (non-neornithine) Mesozoic birds is dominated by enantiornithines, which have been heralded as the first diversification of avialans and are characterized by a range of body sizes and inferred habits[2,14,18–21]. This radiation is notable for its apparent near-global distribution throughout most of the Cretaceous period. An exceptionally well-preserved partial cranium of a previously unknown enantiornithine (University of Antananarivo [UA] 10015) from the latest Cretaceous (Maastrichtian) of Madagascar falls within a critical spatiotemporal gap. Very few avialans are known from the entire Cretaceous period of Afro-Madagascar. The specimen expands our knowledge of realized cranial shape disparity, in terms of both morphological details and the proportions of elements, within the enantiornithine radiation and Mesozoic birds as a whole.

Systematic palaeontology

Theropoda Marsh, 1881
Paraves Sereno, 1997
Avialae Gauthier, 1986
Ornithothoraces Chiappe, 1995
Enantiornithes Walker, 1981
Falcatakely forsterae gen. et sp. nov.

Etymology. '*Falcata*' (from Latin *falcatus*), meaning armed with a scythe, in reference to the shape of the rostrum; '*kely*' (Malagasy), meaning small; '*forsterae*', in recognition of Catherine A. Forster's contributions to work on Madagascan paravians.

Holotype. Partial cranium (University of Antananarivo, UA 10015), which consists of the rostrum, palate and periorbital regions (Fig. 1, Extended Data Figs. 1, 2 and Supplementary Videos 1–8).

[1]Department of Biomedical Sciences, Heritage College of Osteopathic Medicine, Ohio University, Athens, OH, USA. [2]Ohio Center for Ecological and Evolutionary Studies, Ohio University, Athens, OH, USA. [3]Department of Earth Sciences, Denver Museum of Nature & Science, Denver, CO, USA. [4]Department of Anatomical Sciences, Stony Brook University, Stony Brook, NY, USA. [5]Centre for Integrative Anatomy, Department of Cell and Developmental Biology, University College London, London, UK. [6]Geology Department, Macalester College, St Paul, MN, USA. [7]Département de Sciences de la Terre et de l'Environnement, Université d'Antananarivo, Antananarivo, Madagascar. ✉e-mail: oconnorp@ohio.edu

Locality and horizon. Locality MAD05-42, Berivotra Study Area, Upper Cretaceous (Maastrichtian; 72.1–66 million years ago) Anembalemba Member, Maevarano Formation, Mahajanga Basin, northwestern Madagascar[22].

Diagnosis. Differs from other paravians on the basis of the following combination of features (*indicates autapomorphies): extended, high maxilla that forms the dorsal contour of the rostrum*; dimpled texture on the nasal and lacrimal, particularly on the triangular caudodorsal process of the latter*; lacrimal with caudally expanded ventral process*; large, flat jugal process of the postorbital*. Further differs from most avialans by: a long, straight quadratojugal process of the jugal; antorbital fenestra nearly as long as tall. Further differs from other enantiornithines by: premaxilla slots into an extended V-shaped sulcus of the maxilla*; narrow rostrum (width at premaxilla–maxilla junction estimated at around 15% maximum width at rostral margin of orbit); a nasal with distinct fossa near the rostral end*.

Remarks. Avialae and Neornithes are used herein to delimit increasingly less inclusive monophyletic assemblages of theropod dinosaurs. Avialae (that is, birds) refers to all theropods closer to living birds than to dromaeosaurids and troodontids (that is, a stem-based monophyletic group containing *Passer domesticus* and all theropods closer to it than to *Dromaeosaurus* or *Troodon*). Neornithes represents the crown group of birds and is the equivalent of Aves (sensu ref. [23]); see Supplementary Information for additional phylogenetic definitions. Further supporting information (such as interactive PDFs, matrices and executable files) is available on DRYAD (https://doi.org/10.5061/dryad.mkkwh70wg).

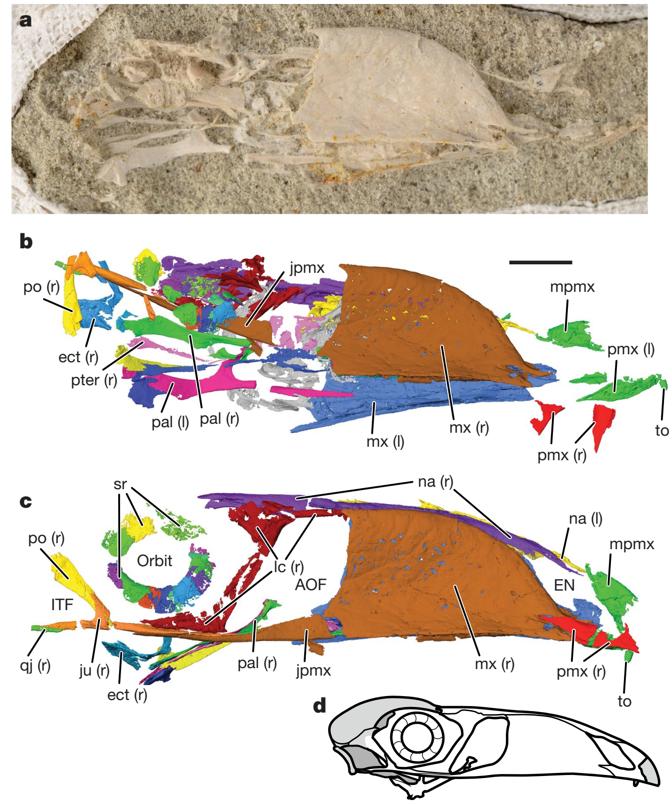

Fig. 1 | Cranium of the Cretaceous enantiornithine bird *Falcatakely forsterae* (UA 10015, holotype). **a**, Photograph of the specimen, with a right lateral view of the pre-orbital region (right side of the image) and a ventral view of the palatal region (left side of the image). **b**, Digital polygon reconstruction from the microcomputed tomography scan of the specimen shown in **a**. **c**, Digital polygon reconstruction of the specimen with most elements in **b** placed in near-life position in right lateral view. Scale bar, 1 cm (**a**–**c**). **d**, Reconstruction (not to scale) illustrating the preserved (in white) elements of the cranium. Left (l) and right (r) sides are indicated. AOF, antorbital fenestra; ect, ectopterygoid; EN, external nares; ITF, infratemporal fenestra; jpmx, jugal process of the maxilla; ju, jugal; lc, lacrimal; mpmx, midline premaxilla; mx, maxilla; na, nasal; pal, palatine; pmx, premaxilla; po, postorbital; pter, pterygoid; qj, quadratojugal; sr, scleral ring; to, tooth.

Cranial osteology

UA 10015 pertains to an enantiornithine bird (estimated cranial length, 8.5 cm) with a high, but extremely narrow, preorbital region (Fig. 1). The lightly built face consists of a long, high edentulous maxilla and a short, tooth-bearing premaxilla, forming a rostrum unlike that of any known bird. The external nares are rostrally positioned and widely separated from a large, parallelogram-shaped antorbital fenestra. The premaxillae are fused rostrally and exhibit a short frontal process as in some other enantiornithines[5,24,25]. The maxillary process is short and slots into a V-shaped concavity on the maxilla (Fig. 1b, c and Extended Data Figs. 1f, 2c). A single, conical, unserrated tooth is preserved in the left premaxilla; the presence of additional premaxillary teeth is uncertain owing to incomplete preservation.

The maxilla of *Falcatakely* is less than 1 mm thick and unique among avialans in being extremely high and long, and forming at least 90% of the reconstructed pre-orbital rostrum height (Fig. 1c). It is unfenestrated, a condition shared with Enantiornithes (Supplementary Information), and lacks an antorbital fossa; it also preserves detailed vascular sulci over its surface that indicate the presence of an expansive keratinous rhamphotheca (beak) in life[26] (Fig. 1a; interactive PDFs can be found at https://doi.org/10.5061/dryad.mkkwh70wg). The premaxillary process is well-developed and forms part of the ventral border of the external naris. An elongate, tapering caudoventral projection contributes to the jugal bar, delimiting the ventral border of the orbit where it underlies the lacrimal boot.

The elongate nasals expand in width caudally and are unique in possessing dorsomedially positioned fossae near the external nares (Extended Data Fig. 1b). The mid-portion of the nasals are broad and vaulted, as in bohaiornithid enantiornithines[5,27] and express surface dimpling on the lateral margin near the articulation with the lacrimal (Extended Data Fig. 1b–d). The reconstruction of *Falcatakely* was generated using microcomputed tomography and reveals a nearly complete right lacrimal (Fig. 1c). The dorsal half of the element is T-shaped, as in avialans such as *Archaeopteryx*, *Pengornis* and *Parapengornis*[2,27]. The rostrodorsal process is considerably longer than the caudodorsal process and is most similar to the condition in pengornithid enantiornithines (for example, *Parapengornis*)[10]. The caudodorsal process is unique among avialans in morphology, being sub-triangular in shape, dimpled and pneumatic (Extended Data Fig. 1d). The ventral ramus is longer than either the caudodorsal or rostrodorsal process, and is extensively excavated, as in pengornithids and bohaiornithids[2,19,27]. The ventral ramus terminates as a caudally expanded boot that sits just dorsal to the overlapping portions of the jugal and maxilla (Fig. 1c).

The jugal is triradiate with a long, dorsoventrally restricted maxillary process, a distinct postorbital process and an extended, bar-like quadratojugal process (Extended Data Fig. 1e). In contrast to most avialans[21,28], the quadratojugal process is long and directed straight caudally, forming the ventral border of the infratemporal fenestra. The quadratojugal process is not bifurcated as in most non-avialan theropods and some phylogenetically early branching birds such as *Sapeornis*[29]. The right postorbital (Extended Data Fig. 1e) is represented only by its ventral process, which is flat and tapering, and is unlike any known among avialans or paravians in general[30]. At least 15 scleral ossicles are present, enough to estimate the external diameter of the scleral ring to be 16–18 mm (Fig. 1c).

The digitally reconstructed palate of UA 10015 (Extended Data Fig. 2) reveals a substantial level of detail not typically observable in Mesozoic

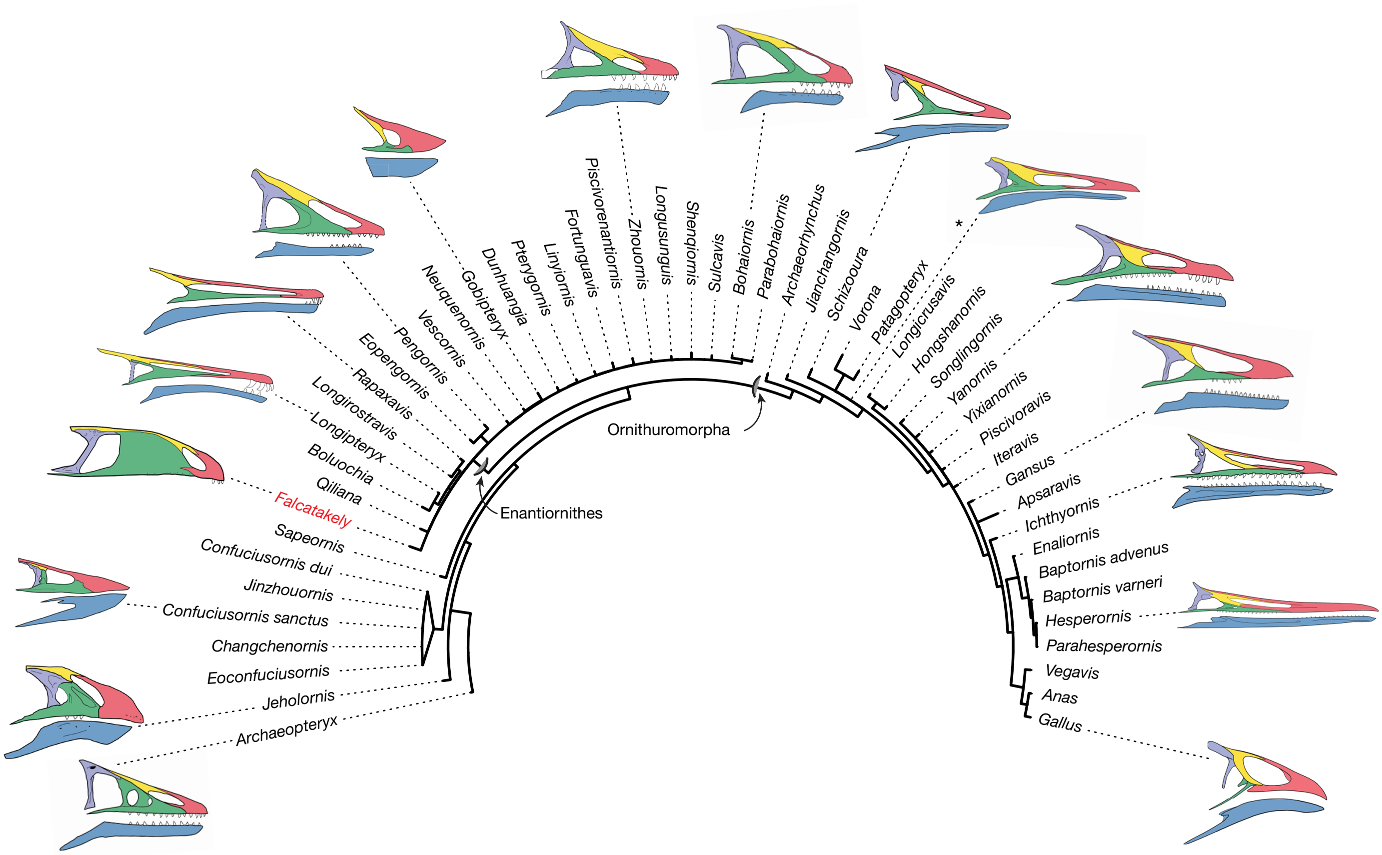

Fig. 2 | Mosaic evolution of the avialan facial skeleton as depicted among select early branching forms. Phylogenetic analysis places *Facatakely* among enantiornithine birds. The illustration of *Xinghaiornis*(*) is placed near its approximate position in the phylogeny based on a previous publication[15]. Illustrations are not to scale. Red, premaxilla; green, maxilla; yellow, nasal; lavender, lacrimal; blue, dentary. Illustrations of *Archaeopteryx*, *Ichthyornis*, *Hesperornis* and *Gallus* were modified from a previous publication[16]. See Supplementary Information for additional details for included taxa and phylogenetic analyses.

avialans. The palatine is triradiate, with a long, thin rostral process that abuts the maxilla (Extended Data Fig. 2a). The palatine does not contact the jugal and only modestly contacts the pterygoid, but shares an elongate contact with the ectopterygoid. A dorsomedially directed choanal process sweeps towards the midline to join its antimere. Only the thin rostral processes of the pterygoids are preserved in UA 10015; these processes are in close association with the palatines (Extended Data Fig. 2a). The ectopterygoid, an element that is unknown in most Cretaceous avialans[24,31], is represented by a robust body and a thin, elongate, uncinate process that contacts the jugal bar (Extended Data Fig. 2a). The vomers are represented by two thin, dorsoventrally restricted laminar plates that extend rostrally between the two maxillae (Extended Data Fig. 2a, c). Thin sheets of bone are present just rostral to the pterygoids, potentially representing the expanded caudal end of the vomer, reminiscent of the condition in *Gobipteryx*[24,31].

Mosaic evolution in the avian beak

Our phylogenetic analyses recover *Falcatakely* nested within Enantiornithes (Fig. 2 and Extended Data Figs. 3, 4). The long, deep and narrow rostrum of *Falcatakely*, dominated by an expanded maxilla, provides a stark contrast to the facial region formed by the premaxilla and maxilla in other enantiornithines and more-crownward non-neornithines. Even among rostrally elongated ornithothoracine taxa such as *Longipteryx*, *Longirostravis* and *Dingavis*, this morphology is achieved through a concomitant reduction in premaxillary and maxillary height as bones elongate along the rostrocaudal axis[5,6,12,14,15].

Quantitative assessment of non-avialan and avialan (including Neornithes) facial shape demonstrates the combination of a derived cranial phenotype in *Falcatakely* (that is, a neornithine-like expanded rostrum) formed by an underlying plesiomorphic paravian skeletal framework. We used two-dimensional geometric morphometrics (Fig. 3) to compare the maxillary and premaxillary shape in UA 10015 to that of a sample of fossil non-avialan theropods, as well as the crown birds *Gallus gallus* (red junglefowl) and *Nothoprocta pentlandii* (Andean tinamou). Principal component analysis reveals that species group together on the basis of the ratio of the maxillary to premaxillary size (the first principal component) and the ratio of the rostrocaudal length to dorsoventral height of both elements (second principal component). Despite having maxillary and premaxillary proportions that are similar to those of non-avialan theropods (for example, paravians, oviraptorosaurs and ornithomimosaurs), *Falcatakely* exhibits an overall rostrum phenotype that is convergent on a number of neornithine groups.

The configuration of the individual skeletal elements in *Falcatakely* is more similar to the non-avialans *Microraptor* and *Zanabazar* than to ornithuromorphs (including neornithines) owing to the expanded maxilla and relatively small premaxilla. Nonetheless, the three-dimensional shape of the pre-orbital facial skeleton closely resembles that of some extant birds (Extended Data Figs. 5, 6), as assessed using three-dimensional geometric morphometrics to compare the shape of the maxilla, premaxilla and nasal within a sample of 349 extant birds[32] (Supplementary Information). Principal component analysis of the rostrum shape reveals that *Falcatakely* occupies a position in whole-rostrum morphospace that is quantitatively similar to those

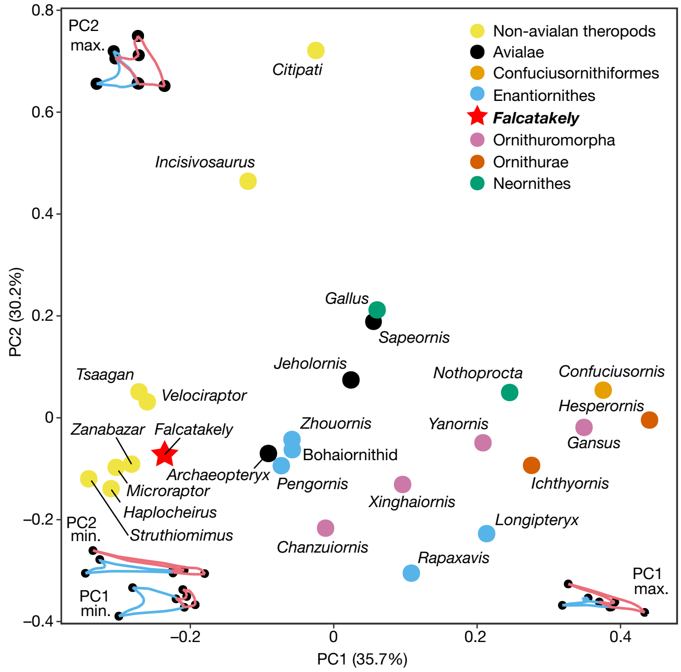

Fig. 3 | Geometric morphometric analyses of the facial shape of *Falcatakely* among paravians. Plot of the first two principal components (PCs) of the two-dimensional landmark analysis of maxillary (blue line segments) and premaxillary (red line segments) morphology of select theropod taxa. The configuration of maxilla and premaxilla in *Falcatakely* is more similar to that of non-avialans in a two-dimensional analysis focused on fossil taxa, although the overall three-dimensional rostrum phenotype occupies a morphospace converged on by subsequent radiations of neornithine birds (Supplementary Data). See Supplementary Information for analytical protocols.

of a number of unrelated neornithines, including members of the Ramphastidae (toucans), Phaethonidae (tropicbirds), Columbidae (pigeons and doves) and Tyrannidae (tyrant flycatchers) (an interactive morphospace plot is included as Supplementary Data and at https://doi.org/10.5061/dryad.mkkwh70wg).

The discovery of *Falcatakely* expands the realized cranial morphology among known non-neornithine birds considerably. Analysis of its three-dimensional anatomy shows that it is a stem bird that occupies a previously unrealized position in rostrum morphospace and potentially exploited an ecology that was not again seen until the diversification of crown-group birds in the mid-Cenozoic era. A partial emancipation of the palate from the facial skeleton (that is, loss of jugal contact with the palatine) concurrent with heretofore unappreciated rostrum elaboration suggests that these regions are functionally and developmentally integrated[16,31,33]. Notably, a mosaic pattern of palatal release is found among stem avialans, at least insofar as the functional demands of the rostrum or beak in *Falcatakely* appears to have required reinforcement of the connections to the rear of the face. These connections are maintained through the ectopterygoid and with retention of the robust postorbital linkage, despite the loss of the mid-face palatine connection to the jugal bar. Such an arrangement was probably necessary to stabilize the mid-portion of the cranium and the long, high and extremely narrow rostrum. Although incomplete, the presence of a robust postorbital further indicates a rigidly enforced caudal region of the cranium[7].

The maxilla-dominated facial skeleton of *Falcatakely* reveals two important insights for the evolutionary history of birds. First, the ancestral developmental patterning of rostrum construction in basal avialans has generated neornithine-like cranial phenotypes that have not been recognized in the fossil record until now. Second, the developmental reduction of the maxilla previously inferred for Ornithothoraces[7,9] was not a fixed trait, at least among enantiornithine birds. Thus, consolidation to a premaxilla-dominated rostrum, a hallmark of all living birds, was not an evolutionary prerequisite for rostrum and, therefore, beak enlargement. More generally, this is consistent with a growing appreciation of the flexibility of the underlying developmental mechanisms[8,34,35] that may be responsible for the generation of convergent morphologies among distantly related forms. With *Falcatakely*, this appreciation can now be extended to the deep-time avialan record. The discovery of *Falcatakely* expands the ecomorphological potential realized by enantiornithines and Mesozoic birds more generally[3,18]. This new appreciation of avialan anatomy underscores the potential for considerable variability in trophic ecology during the first great diversification of the group during the Cretaceous period[5,6,36,37].

Online content

Any methods, additional references, Nature Research reporting summaries, source data, extended data, supplementary information, acknowledgements, peer review information; details of author contributions and competing interests; and statements of data and code availability are available at https://doi.org/10.1038/s41586-020-2945-x.

1. Xu, X. et al. An integrative approach to understanding bird origins. *Science* **346**, 1253293 (2014).
2. Zhou, Z., Clarke, J. & Zhang, F. Insight into diversity, body size and morphological evolution from the largest Early Cretaceous enantiornithine bird. *J. Anat.* **212**, 565–577 (2008).
3. Brusatte, S. L., O'Connor, J. K. & Jarvis, E. D. The origin and diversification of birds. *Curr. Biol.* **25**, R888–R898 (2015).
4. O'Connor, J. K. in *The Evolution of Feathers* (eds Foth, C. & Rauhut, O. W. M.) 147–172 (Springer, 2020).
5. O'Connor, J. K. & Chiappe, L. M. A revision of enantiornithine (Aves: Ornithothoraces) skull morphology. *J. Syst. Palaeontol.* **9**, 135–157 (2011).
6. Huang, J. et al. A new ornithurine from the Early Cretaceous of China sheds light on the evolution of early ecological and cranial diversity in birds. *PeerJ* **4**, e1765 (2016).
7. Bhullar, B.-A. S. et al. How to make a bird skull: major transitions in the evolution of the avian cranium, paedomorphosis, and the beak as a surrogate hand. *Integr. Comp. Biol.* **56**, 389–403 (2016).
8. Young, N. M. et al. Embryonic bauplans and the developmental origins of facial diversity and constraint. *Development* **141**, 1059–1063 (2014).
9. Mayr, G. Comparative morphology of the avian maxillary bone (os maxillare) based on an examination of macerated juvenile skeletons. *Acta Zool.* **101**, 24–38 (2020).
10. Hu, H., O'Connor, J. K. & Zhou, Z. A new species of Pengornithidae (Aves: Enantiornithes) from the Lower Cretaceous of China suggests a specialized scansorial habitat previously unknown in early birds. *PLoS ONE* **10**, e0126791 (2015).
11. Bailleul, A. M. et al. An Early Cretaceous enantiornithine (Aves) preserving an unlaid egg and probable medullary bone. *Nat. Commun.* **10**, 1275 (2019).
12. Hou, L., Chiappe, L. M., Zhang, F. & Chuong, C.-M. New Early Cretaceous fossil from China documents a novel trophic specialization for Mesozoic birds. *Naturwissenschaften* **91**, 22–25 (2004).
13. O'Connor, J. K. et al. Phylogenetic support for a specialized clade of Cretaceous enantiornithine birds with information from a new species. *J. Vertebr. Paleontol.* **29**, 188–204 (2009).
14. O'Connor, J. K., Chiappe, L. M., Gao, C. & Zhao, B. Anatomy of the Early Cretaceous enantiornithine bird *Rapaxavis pani*. *Acta Palaeontol. Pol.* **56**, 463–475 (2011).
15. O'Connor, J. K., Wang, M. & Hu, H. A new ornithuromorph (Aves) with an elongate rostrum from the Jehol Biota, and the early evolution of rostralization in birds. *J. Syst. Palaeontol.* **14**, 939–948 (2016).
16. Field, D. J. et al. Complete *Ichthyornis* skull illuminates mosaic assembly of the avian head. *Nature* **557**, 96–100 (2018).
17. Field, D. J., Benito, J., Chen, A., Jagt, J. W. M. & Ksepka, D. T. Late Cretaceous neornithine from Europe illuminates the origins of crown birds. *Nature* **579**, 397–401 (2020).
18. Chiappe, L. M. & Witmer, L. M. *Mesozoic Birds: Above the Heads of Dinosaurs* (Univ. California Press, 2004).
19. Li, Z., Zhou, Z., Wang, M. & Clarke, J. A. A new specimen of large-bodied basal enantiornithine *Bohaiornis* from the Early Cretaceous of China and the inference of feeding ecology in Mesozoic birds. *J. Paleontol.* **88**, 99–108 (2014).
20. Wang, M., Hu, H. & Li, Z. A new small enantiornithine bird from the Jehol Biota, with implications for early evolution of avian skull morphology. *J. Syst. Palaeontol.* **14**, 481–497 (2016).
21. Wang, M., O'Connor, J. K. & Zhou, Z. A new robust enantiornithine bird from the Lower Cretaceous of China with scansorial adaptations. *J. Vertebr. Paleontol.* **34**, 657–671 (2014).
22. Rogers, R. R., Hartman, J. H. & Krause, D. W. Stratigraphic analysis of Upper Cretaceous rocks in the Mahajanga Basin, northwestern Madagascar: implications for ancient and modern faunas. *J. Geol.* **108**, 275–301 (2000).
23. Gauthier, J. A. & de Queiroz, K. in *New Perspectives on the Origin and Early Evolution of Birds: Proceedings of the International Symposium in Honor of John H. Ostrom* (eds Gauthier, J. & Gall, L. F.). 7–41 (Peabody Museum of Natural History, Yale Univ., 2001).

24. Chiappe, L. M., Norell, M. A. & Clark, J. M. A new skull of *Gobipteryx minuta* (Aves: Enantiornithes) from the Cretaceous of the Gobi Desert. *Am. Mus. Novit*. **3346**, 1–15 (2001).
25. Wang, M. & Zhou, Z. A new enantiornithine (Aves: Ornithothoraces) with completely fused premaxillae from the Early Cretaceous of China. *J. Syst. Palaeontol*. **17**, 1299–1312 (2019).
26. Hieronymus, T. L. & Witmer, L. M. Homology and evolution of avian compound Rhamphothecae. *Auk* **127**, 590–604 (2010).
27. Wang, M., Zhou, Z.-H., O'Connor, J. K. & Zelenkov, N. V. A new diverse enantiornithine family (Bohaiornithidae fam. nov.) from the Lower Cretaceous of China with information from two new species. *Vert. Palasiat*. **52**, 31–76 (2014).
28. Wang, M. & Hu, H. A comparative morphological study of the jugal and quadratojugal in early birds and their dinosaurian relatives. *Anat. Rec*. **300**, 62–75 (2017).
29. Wang, Y. et al. A previously undescribed specimen reveals new information on the dentition of *Sapeornis chaoyangensis*. *Cretac. Res*. **74**, 1–10 (2017).
30. Hu, H., O'Connor, J. K., Wang, M., Wroe, S. & McDonald, P. G. New anatomical information on the bohaiornithid *Longusunguis* and the presence of a plesiomorphic diapsid skull in Enantiornithes. *J. Syst. Palaeontol*. **18**, 1481–1495 (2020).
31. Hu, H. et al. Evolution of the vomer and its implications for cranial kinesis in Paraves. *Proc. Natl Acad. Sci. USA* **116**, 19571–19578 (2019).
32. Felice, R. N. & Goswami, A. Developmental origins of mosaic evolution in the avian cranium. *Proc. Natl Acad. Sci. USA* **115**, 555–560 (2018).
33. Bhullar, B.-A. S. et al. A molecular mechanism for the origin of a key evolutionary innovation, the bird beak and palate, revealed by an integrative approach to major transitions in vertebrate history. *Evolution* **69**, 1665–1677 (2015).
34. Mallarino, R. et al. Closely related bird species demonstrate flexibility between beak morphology and underlying developmental programs. *Proc. Natl Acad. Sci. USA* **109**, 16222–16227 (2012).
35. Tokita, M., Yano, W., James, H. F. & Abzhanov, A. Cranial shape evolution in adaptive radiations of birds: comparative morphometrics of Darwin's finches and Hawaiian honeycreepers. *Phil. Trans. R. Soc. Lond. B* **372**, 20150481 (2017).
36. Bell, A. & Chiappe, L. M. Statistical approaches for inferring ecology in Mesozoic birds. *J. Syst. Palaeontol*. **9**, 119–133 (2011).
37. O'Connor, J. K. The trophic habits of early birds. *Palaeogeogr. Palaeoclimatol. Palaeoecol*. **513**, 178–195 (2019).

Methods

Temporal and stratigraphic context

UA 10015 was recovered in 2010 at the locality MAD05-42 in the Berivotra Study Area of the Mahajanga Basin Project. The bone-bearing horizon lies within facies 2 of the Anembalemba Member in the Upper Cretaceous (Maastrichtian) Maevarano Formation[22] (Supplementary Information). Many specimens—including UA 10015—that were recovered from the Anembalemba Member were entombed by debris flows, which often results in high-quality preservation with only minimal displacement and taphonomic distortion during burial[38,39].

Phylogenetic methods

Given the extremely derived condition in *Falcatakely* and the notable amount of homoplasy among non-avialan paravians and basal avialans, we used a two-tiered dataset approach in an effort to best constrain the phylogenetic affinities of *Falcatakely* (Supplementary Information). First, we used the densely sampled, coelurosaur-wide matrix from the Theropod Working Group (TWiG)[40,41] to broadly assess and confirm the position of *Falcatakely* among paravians (Extended Data Fig. 3 and Supplementary Information). Next, we used a modified version of a well-established Mesozoic avialan-focused (WEA) matrix[25], along with previously described modifications[16], to further examine the relationship of *Falcatakely* among avialans (Fig. 2 and Extended Data Fig. 4). Bayesian inference trees were estimated for each dataset using MrBayes v.3.2[42]. The standard model (Markov *k*-state variable model)[43] was specified with gamma-distributed rate variation[44]. A subset of characters was set as ordered, following the previous use of the included datasets. During the analysis, Markov chain Monte Carlo convergence was assessed using the average standard deviation of split frequencies and by examining the trace files in Tracer[45]. Convergence to stationarity was assumed for split frequencies below 0.01 and effective sample size values >200. All analyses were performed with two runs of four chains each that were run for 10 million generations while sampling parameters every 1,000 generations. The first 25% of samples were discarded as burn-in. Results are summarized using a majority rule consensus (MRC) tree[46]. MRC trees for both datasets depict *Falcatakely* as a member of Enantiornithes. The TWiG dataset recovers *Falcatakely* as the sister taxon to *Pengornis*, whereas the WEA matrix finds *Falcatakely* in a large polytomy with other enantiornithines (Extended Data Figs. 3, 4). Given the denser avialan sampling in the WEA dataset, the phylogenetic results from this matrix are used here as the primary results. Clade support was assessed using the estimated posterior probabilities from the Bayesian inference trees. Morphological character support was established for the MRC trees using the map and apo commands in TNT[47–49]. Additional details for the phylogenetic results and clade support are presented in the Supplementary Information.

To further investigate the robustness of our inferred trees, three sensitivity analyses were performed examining the influence of cranial versus postcranial data and of cranial-only character scorings for select taxa (for example, *Archaeopteryx* and *Sapeornis*) on tree inference. These analyses reveal no significant topological alterations relative to the standard analysis described above, lending support to the primary results in which *Falcatakely* is placed among enantiornithine birds. Moreover, additional explicit hypothesis testing using Bayes factor comparisons was conducted with *Falcatakely* constrained to stemward positions (for example, with *Falcatakely* excluded from Pygostylia), which resulted in suboptimal solutions. Details for these analyses and the specifics of the results are provided in the Supplementary Information; executable files for the sensitivity and alternative hypothesis testing are available on DRYAD (https://doi.org/10.5061/dryad.mkkwh70wg).

Reporting summary

Further information on research design is available in the Nature Research Reporting Summary linked to this paper.

Data availability

UA 10015 is catalogued into the collections at the Université d'Antananarivo. Details regarding the development of the digital files and the derivatives of these files (such as DICOM or PLY) used as part of the study are included in the Supplementary Information and archived on the MorphoSource website (https://www.morphosource.org/Detail/ProjectDetail/Show/project_id/7894). Phylogenetic character information and parameters used in the analyses are provided in the Supplementary Information. Executable files for phylogenetic analyses, character–taxon matrices, an interactive three-dimensional morphospace plot and interactive three-dimensional PDFs are hosted on DRYAD (https://doi.org/10.5061/dryad.mkkwh70wg). This published study, including the novel genus (urn:lsid:zoobank.org:act:5BA26059-B428-4896-BFEA-2475419C61FC) and species (urn:lsid:zoobank.org:act:69314771-F0D8-4C15-946C-524164385FB7) along with the associated nomenclatural acts, have been registered in ZooBank: urn:lsid:zoobank.org:pub:4595D69E-FE12-4DAD-B155-89F084254F73.

38. Rogers, R. R. Fine-grained debris flows and extraordinary vertebrate burials in the Late Cretaceous of Madagascar. *Geology* **33**, 297–300 (2005).
39. Rogers, R. R., Krause, D. W., Curry Rogers, K., Rasoamiaramanana, A. H. & Rahantarisoa, L. Paleoenvironment and paleoecology of *Majungasaurus crenatissimus* (Theropoda: Abelisauridae) from the Late Cretaceous of Madagascar. *J. Vertebr. Paleontol*. **27**, 21–31 (2007).
40. Brusatte, S. L., Lloyd, G. T., Wang, S. C. & Norell, M. A. Gradual assembly of avian body plan culminated in rapid rates of evolution across the dinosaur–bird transition. *Curr. Biol.* **24**, 2386–2392 (2014).
41. Turner, A. H., Makovicky, P. J. & Norell, M. A. A review of dromaeosaurid systematics and paravian phylogeny. *Bull. Am. Mus. Nat. Hist*. **371**, 1–206 (2012).
42. Ronquist, F. et al. MrBayes 3.2: efficient Bayesian phylogenetic inference and model choice across a large model space. *Syst. Biol*. **61**, 539–542 (2012).
43. Lewis, P. O. A likelihood approach to estimating phylogeny from discrete morphological character data. *Syst. Biol*. **50**, 913–925 (2001).
44. Clarke, J. A. & Middleton, K. M. Mosaicism, modules, and the evolution of birds: results from a Bayesian approach to the study of morphological evolution using discrete character data. *Syst. Biol*. **57**, 185–201 (2008).
45. Rambaut, A., Suchard, M. A., Xie, D. & Drummond, A. J. Tracer v.1.6. http://beast.community/tracer (2014).
46. O'Reilly, J. E. & Donoghue, P. C. J. The efficacy of consensus tree methods for summarizing phylogenetic relationships from a posterior sample of trees estimated from morphological data. *Syst. Biol*. **67**, 354–362 (2018).
47. Goloboff, P. A., Farris, J. & Nixon, K. TNT, a free program for phylogenetic analysis. *Cladistics* **24**, 774–786 (2008).
48. Goloboff, P. A., Farris, J. S. & Nixon, K. C. TNT: tree analysis using new technology. version 1.1 (Willi Hennig Society Edition) http://www.lillo.org.ar/phylogeny/tnt/ (2008).
49. Goloboff, P. A. & Catalano, S. A. TNT version 1.5, including a full implementation of phylogenetic morphometrics. *Cladistics* **32**, 221–238 (2016).

Acknowledgements We thank the Université d'Antananarivo, the Mahajanga Basin Project field teams and the villagers of the Berivotra Study Area for support; the ministries of Mines, Higher Education and Culture of the Republic of Madagascar for permission to conduct field research; the National Geographic Society (8597-09) and the US National Science Foundation (EAR–0446488, EAR–1525915, EAR–1664432) for funding; and M. Witton for drafting the line drawings used in Fig. 1 and Extended Data Figs. 1, 2. Collection of avian three-dimensional morphometric data was funded by European Research Council grant no. STG-2014-637171 (to A. Goswami). Full acknowledgments are provided in the Supplementary Information.

Author contributions P.M.O., A.H.T. and J.R.G. designed the project; P.M.O., A.H.T., J.R.G., R.R.R., D.W.K. and L.J.R. conducted the fieldwork. J.R.G. performed the mechanical preparation of the specimen; J.R.G. and P.M.O. conducted the digital preparation and interpretation of the specimen using microcomputed tomography and carried out the rapid prototyping of UA 10015; R.R.R. and L.J.R. provided geological data and taphonomic interpretation; P.M.O., A.H.T., J.R.G. and R.N.F. completed the laboratory work on and digital representation of the fossil and provided input on descriptions and comparisons; A.H.T. and P.M.O. contributed to the character coding and phylogenetic analysis; R.N.F. completed the morphometric analyses; P.M.O., A.H.T. and J.R.G. developed the manuscript, with contributions and/or editing from all authors.

Competing interests The authors declare no competing interests.

Additional information

Supplementary information is available for this paper at https://doi.org/10.1038/s41586-020-2945-x.

Correspondence and requests for materials should be addressed to P.M.O.

Peer review information *Nature* thanks Bhart-Anjan Bhullar and Daniel Field for their contribution to the peer review of this work.

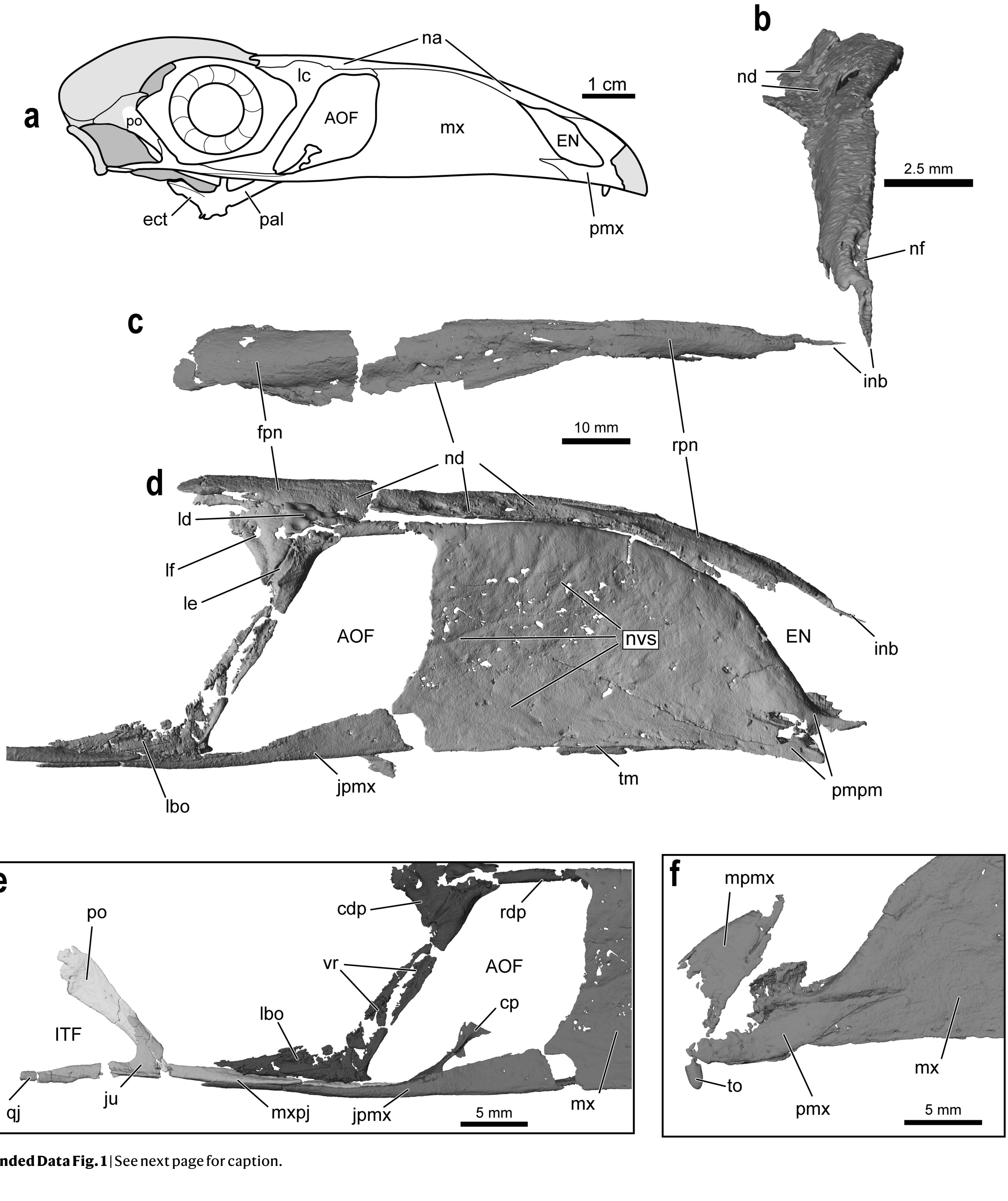

Extended Data Fig. 1 | See next page for caption.

Extended Data Fig. 1 | Rostrum of the Cretaceous enantiornithine bird *Falcatakely* (UA 10015, holotype). **a**, Reconstruction (not to scale) illustrating the preserved (in white) elements of the cranium. **b**, Digital polygon surface reconstruction (from microcomputed tomography scans) of the right nasal in rostrodorsal view (caudal to the top) highlighting the midline depression and dimpled surface texture. **c**, Digital polygon surface reconstruction of the right nasal in dorsal view illustrating the dimpled architecture on the frontal and rostral portions, which extends laterally onto the lacrimal. **d**, Digital polygon surface reconstruction of the right facial elements in right lateral view to illustrate the shape and inter-element relationships of the nasal, maxilla and lacrimal (note the surface texture of the right maxilla with neurovascular sulci broadly expressed over the lateral surface, deep to the inferred keratinous covering (that is, beak)). **e**, Digital polygon surface reconstruction of the lower lateral face to highlight arrangement of the maxilla, lacrimal, jugal and postorbital (all elements from the right side). **f**, Digital polygon surface reconstruction of left maxilla and premaxilla articulation (rostral to the left). AOF, antorbital fenestra; cdp, caudodorsal process of the lacrimal; cp, choanal process of the palatine; ect, ectopterygoid; EN, external nares; ITF, infratemporal fenestra; fpn, frontal process of the nasal; inb, internarial bar; jpmx, jugal process of the maxilla; ju, jugal; lbo, lacrimal boot; lc, lacrimal; ld, lacrimal dimpling; le, lacrimal excavation; lf, lacrimal foramen; mpmx, midline premaxilla; mx, maxilla; mxpj, maxillary process of the jugal; na, nasal; nd, nasal dimpling; nf, nasal fossa; nvs, neurovascular sulci; pal, palatine; pmpm, premaxillary process of the maxilla; pmx, premaxilla; po, postorbital; qj, quadratojugal; rdp, rostrodorsal process of the lacrimal; rpn, rostral process of the nasal; tm, tomial margin; to, tooth; vr, ventral ramus of the lacrimal.

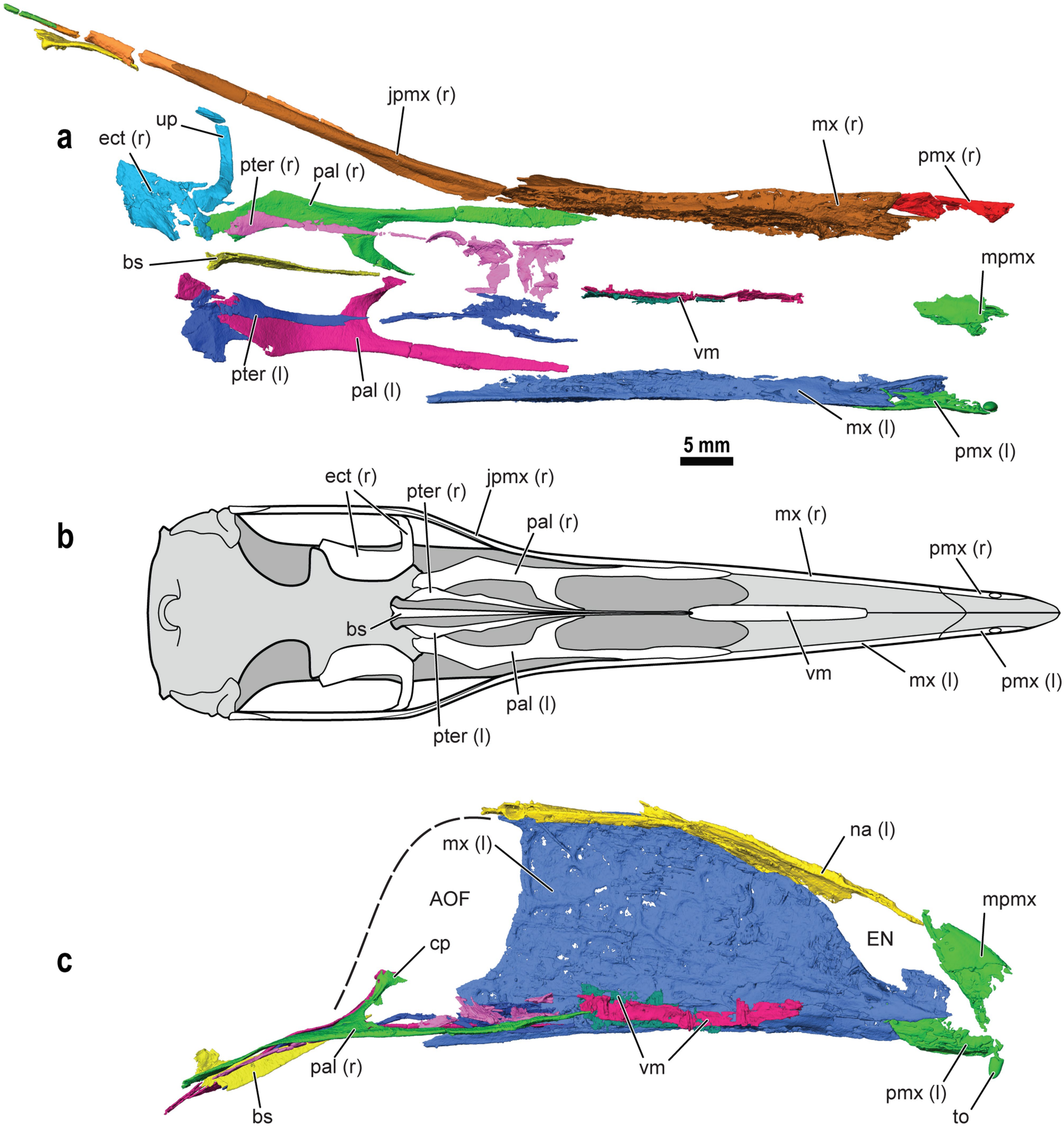

Extended Data Fig. 2 | Palatal and lateral facial regions of the Cretaceous enantiornithine bird *Falcatakely* (UA 10015, holotype). **a**, Digital polygon surface reconstruction (from microcomputed tomography scans) of the palate and lateral face in ventral view. **b**, Reconstructed outline drawing of *Falcatakely* in palatal view (shaded regions are not preserved). **c**, Digital polygon surface reconstruction of internal aspect of left facial skeleton (premaxilla, maxilla and nasal) and palate in right lateral view. The left and right sides are indicated as (l) and (r), respectively. The dashed line in **c** represents the approximate contour of the caudal margin (that is, the ventral ramus of the lacrimal) of the antorbital fenestra. Scale bar, 5 mm; the scale bar is representative for **a** and **c**; the reconstruction in **b** is not to the same scale. AOF, antorbital fenestra; bs, basisphenoid rostrum; cp, choanal process of the (right) palatine; ect, ectopterygoid; EN, external nares; jpmx, jugal process of the maxilla; mpmx, midline premaxilla; mx, maxilla; na, nasal; pal, palatine; pmx, premaxilla; pter, pterygoid; to, tooth; up, uncinate process of the ectopterygoid; vm, vomers.

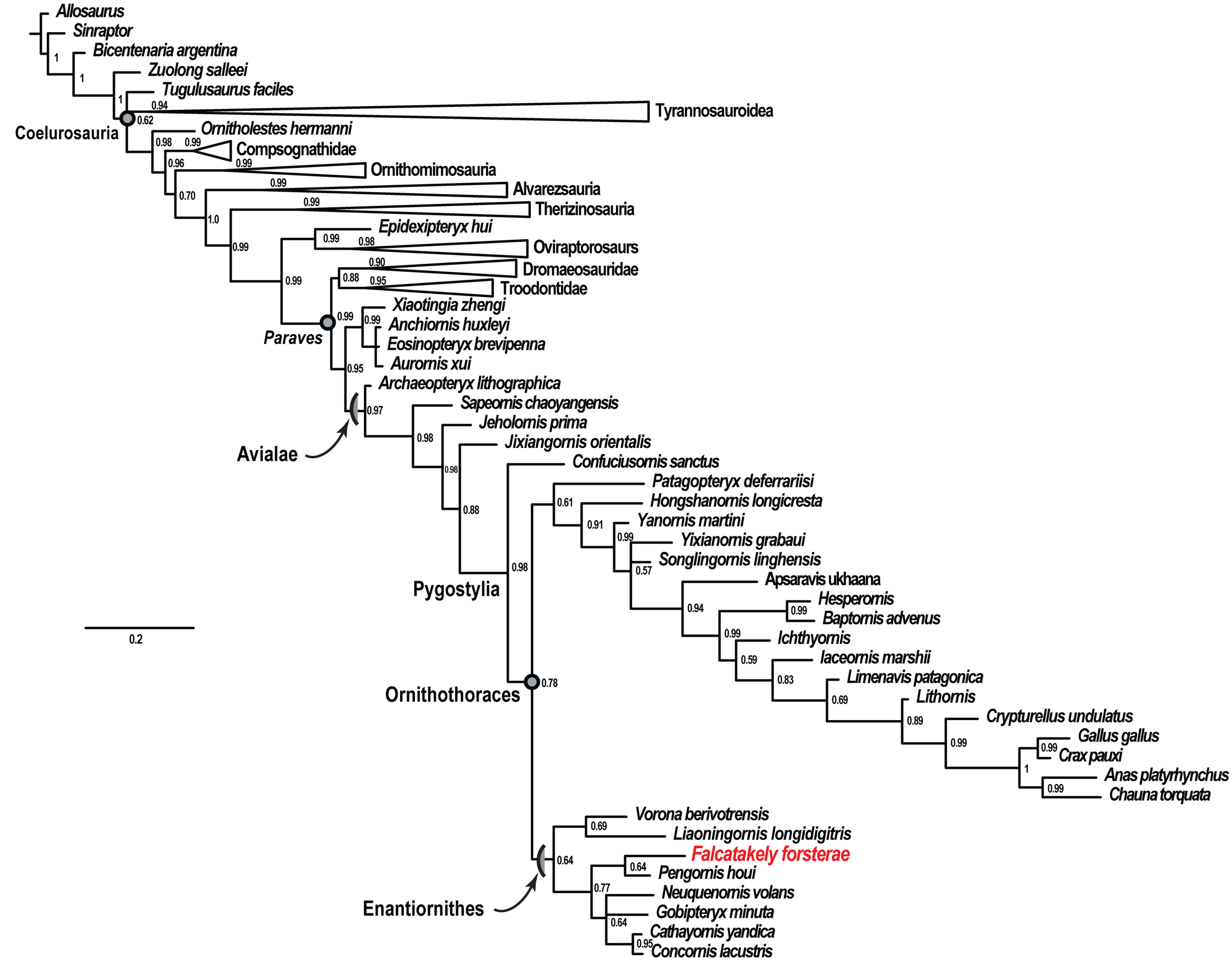

Extended Data Fig. 3 | Majority- rule tree of *Falcatakely* among coelurosaurians from the Bayesian analysis of the TWiG matrix. Clades outside of the Avialae are collapsed for brevity. Posterior probabilities are placed above the nodes.

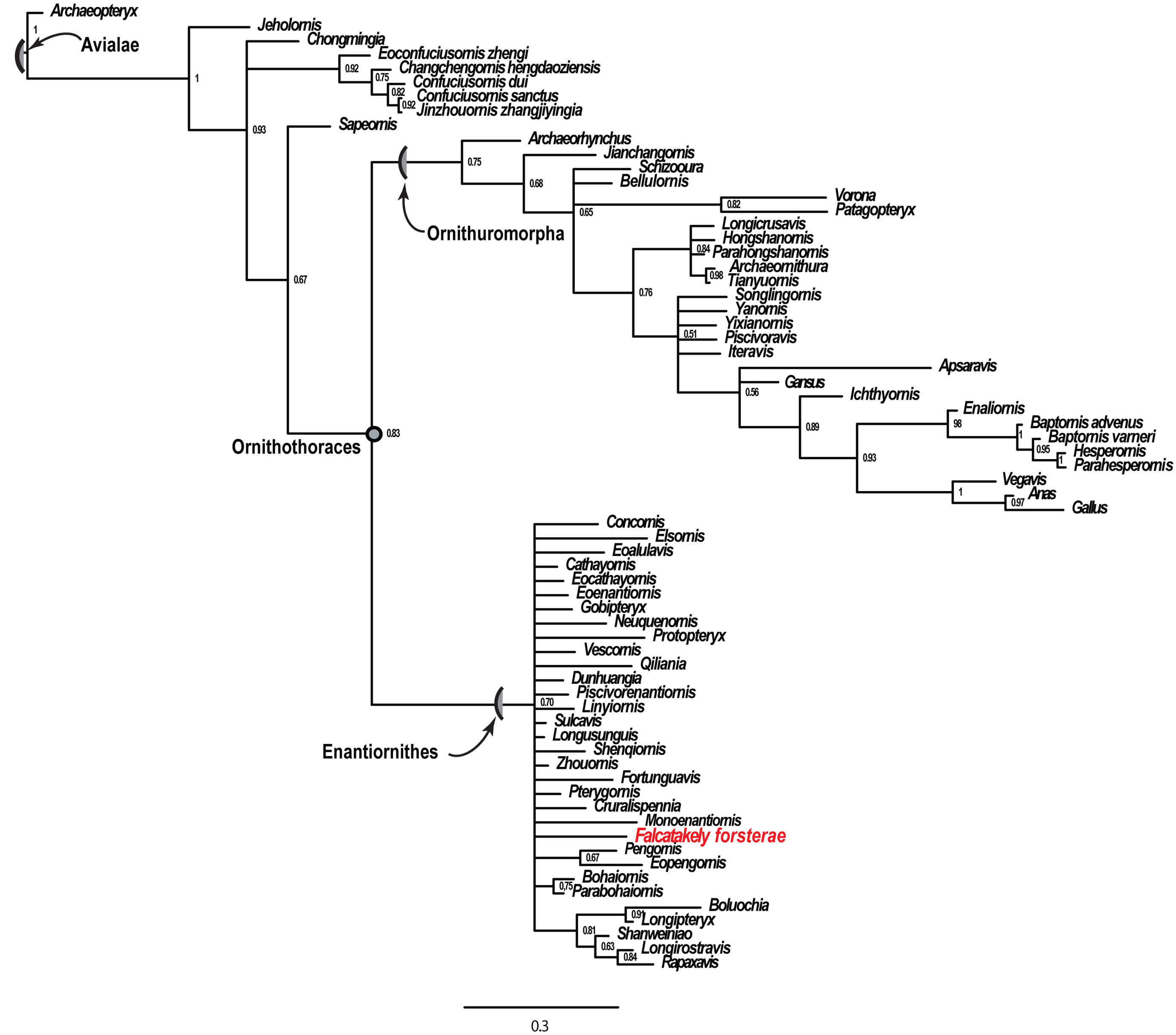

Extended Data Fig. 4 | Majority-rule tree of *Falcatakely* among avialans from the Bayesian analysis of a modified matrix that was previously published. A matrix modified from a previous study[25] was used. Posterior probabilities are placed above the nodes.

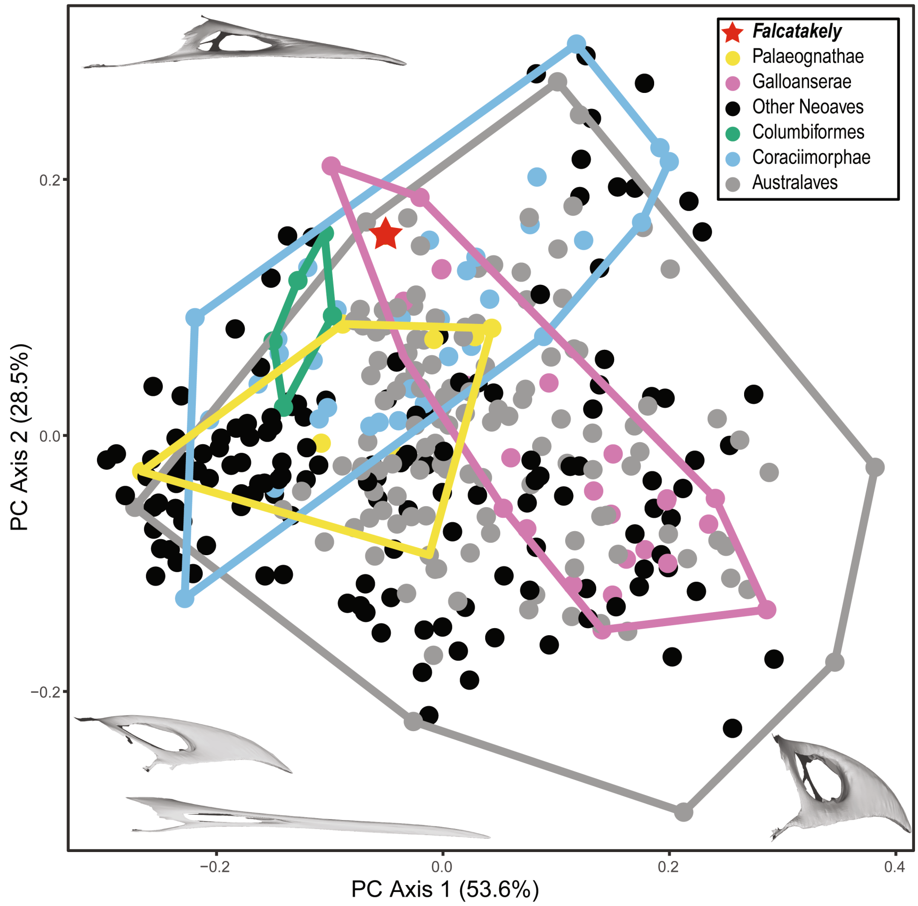

Extended Data Fig. 5 | Geometric morphometric analysis of rostrum shape in *Falcatakely* among avians. Plot of the first two principal components of the three-dimensional landmark analysis of total rostrum shape of *Falcatakely* and extant avian taxa. Whereas the unique configuration of the maxilla and premaxilla in *Falcatakely* is more similar to those of non-avialan paravians (Fig. 3), the overall three-dimensional rostrum phenotype occupies the morphospace that is converged on by subsequent radiations of neornithine birds (Supplementary Data). See Supplementary Information for analytical protocols.

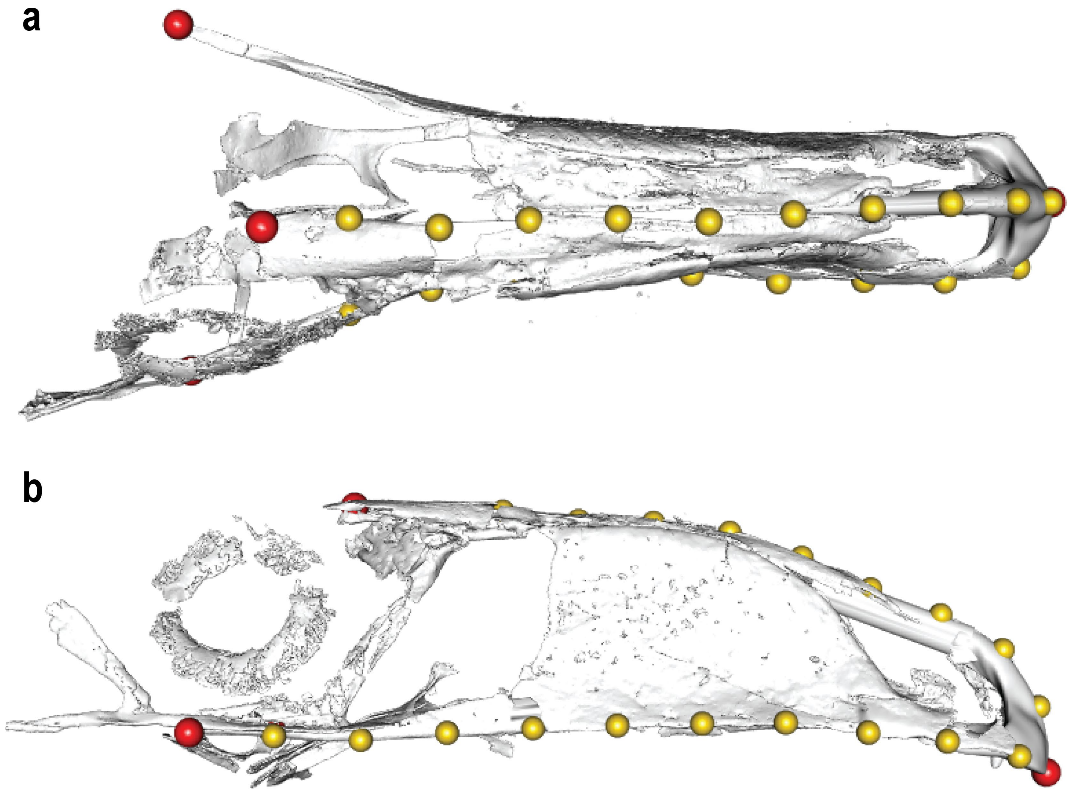

Extended Data Fig. 6 | Landmarking procedure for three-dimensional geometric morphometric analysis in dorsal and lateral views. a, Dorsal view. **b**, Lateral view. Red spheres represent anatomical (type I) landmarks; yellow spheres are sliding semi-landmarks.

nature research

Corresponding author(s): Patrick M. O'Connor

Last updated by author(s): Aug 17, 2020

Reporting Summary

Nature Research wishes to improve the reproducibility of the work that we publish. This form provides structure for consistency and transparency in reporting. For further information on Nature Research policies, see our Editorial Policies and the Editorial Policy Checklist.

Statistics

For all statistical analyses, confirm that the following items are present in the figure legend, table legend, main text, or Methods section.

n/a	Confirmed	
☒	☐	The exact sample size (n) for each experimental group/condition, given as a discrete number and unit of measurement
☒	☐	A statement on whether measurements were taken from distinct samples or whether the same sample was measured repeatedly
☒	☐	The statistical test(s) used AND whether they are one- or two-sided *Only common tests should be described solely by name; describe more complex techniques in the Methods section.*
☒	☐	A description of all covariates tested
☒	☐	A description of any assumptions or corrections, such as tests of normality and adjustment for multiple comparisons
☐	☒	A full description of the statistical parameters including central tendency (e.g. means) or other basic estimates (e.g. regression coefficient) AND variation (e.g. standard deviation) or associated estimates of uncertainty (e.g. confidence intervals)
☒	☐	For null hypothesis testing, the test statistic (e.g. F, t, r) with confidence intervals, effect sizes, degrees of freedom and P value noted *Give P values as exact values whenever suitable.*
☐	☒	For Bayesian analysis, information on the choice of priors and Markov chain Monte Carlo settings
☒	☐	For hierarchical and complex designs, identification of the appropriate level for tests and full reporting of outcomes
☒	☐	Estimates of effect sizes (e.g. Cohen's d, Pearson's r), indicating how they were calculated

Our web collection on statistics for biologists contains articles on many of the points above.

Software and code

Policy information about availability of computer code

Data collection	Avizo 7.1 (VSG), 9.2 (FEI/Thermo-Fisher Scientific), and Avizo Lite 2019 (ThermoScientific); ImageJ v1.48 (National Institutes of Health); Checkpoint (Stratovan); Blender v2.79b.
Data analysis	MrBayes v3.2; TNT 1.5; Tracer v1.6; Geomorph (R package), Adams and Otárola-Castillo, 2013; StereoMorph (R package); Avizo 7 (VSG), 9 (FEI/Thermo-Fisher Scientific), and Avizo Lite 2019 (ThermoScientific); Animation Producer in Avizo; Adobe Acrobat Pro DC (Continuous Release) Version 2020, Adobe Premiere Pro (Creative Cloud edition).

For manuscripts utilizing custom algorithms or software that are central to the research but not yet described in published literature, software must be made available to editors and reviewers. We strongly encourage code deposition in a community repository (e.g. GitHub). See the Nature Research guidelines for submitting code & software for further information.

Data

Policy information about availability of data

All manuscripts must include a data availability statement. This statement should provide the following information, where applicable:

- Accession codes, unique identifiers, or web links for publicly available datasets
- A list of figures that have associated raw data
- A description of any restrictions on data availability

UA 10015 is cataloged into the collections at the Université d'Antananarivo. Details regarding digital file development and derivatives of files (e.g., DICOM, PLY) used as part of the study are included in the Supplementary Information and archived on the MorphoSource website (https://www.morphosource.org/Detail/ProjectDetail/Show/project_id/7894). Phylogenetic character information and parameters used in the analyses are provided in the Supplementary Information. Executable files for phylogenetic analyses, interactive 3D morphospace plot, and interactive 3D PDFs are hosted on DRYAD: https://doi.org/10.5061/dryad.mkkwh70wg. This published work, including the novel genus (urn:lsid:zoobank.org:act:5BA26059-B428-4896-BFEA-2475419C61FC) and species (urn:lsid:zoobank.org:act:69314771-F0D8-4C15-946C-524164385FB7) along with the associated nomenclatural acts, have been registered in ZooBank: urn:lsid:zoobank.org:pub:4595D69E-FE12-4DAD-B155-89F084254F73.

Field-specific reporting

Please select the one below that is the best fit for your research. If you are not sure, read the appropriate sections before making your selection.

☐ Life sciences ☐ Behavioural & social sciences ☒ Ecological, evolutionary & environmental sciences

For a reference copy of the document with all sections, see nature.com/documents/nr-reporting-summary-flat.pdf

Ecological, evolutionary & environmental sciences study design

All studies must disclose on these points even when the disclosure is negative.

Study description	Descriptive/comparative study of a new fossil bird (Falcatakely forsterae) from the Late Cretaceous of Madagascar.
Research sample	This single cranium of Falcatakely (UA 10015) is the only known material of this taxon thus far discovered; it is known exclusively from the Upper Cretaceous (Maastrichtian) of northwestern Madagascar.
Sampling strategy	The study developed herein involves the description of a new taxon based on direct observation, light microscopy, and micro-computed tomography of fossil represented by this single cranium. Digital preparation allowed for the a complete analysis and reconstruction of individual elements of the cranium.
Data collection	The holotype of Falcatakely forsterae (UA 10015) was collected from locality MAD05-42 by hand quarrying (ice pick, brush, rock hammer), with subsequent emplacement in a plaster jacket prior to removal for laboratory processing. Mechanical and digital preparation of the fossil was completed by J.R. Groenke, with interpretation of the anatomy (both of the fossil itself and digital reconstructions/interpretations) by P.M. O'Connor, A.H. Turner, and J.R. Groenke. R.N. Felice led the morphometric analyses included herein. Character scorings assessed by A.H. Turner and P.M. O'Connor, with phylogenetic analyses completed by A.H. Turner.
Timing and spatial scale	The specimen was originally collected during the 2010 calendar year, but only initially prepped and CT scanned (medical CT scanner of the plaster jacket) that same year, yielding an ambiguous identification. J.R. Groenke (Ohio University) did additional mechanical preparation in March 2017, immediately followed by a high-resolution microCT scan in April 2017. Intensive digital preparation then ensued between April 2017 and January 2018, with subsequent, albeit intermittent, digital preparation, interpretation and refinement of models through January 2019.
Data exclusions	No data were excluded.
Reproducibility	Not applicable; given that this paper focuses on a single specimen thus far known to humankind, it does not fall into the category for being reproducible. However, the datasets assembled for this study are publicly available for future reanalyses by other workers.
Randomization	Not Applicable.
Blinding	Not applicable

Did the study involve field work? ☒ Yes ☐ No

Field work, collection and transport

Field conditions	Fieldwork was conducted during the austral summer (i.e., the dry season) in 2010 in the Mahajanga Basin, near the village of Berivotra, Madagascar.
Location	The holotypic specimen was collected from the Upper Cretaceous Maevarano Formation, Mahajanga Basin, Madagascar. Approximate coordinates: S 15 degrees, 54' 20.94", E 46 degrees, 35' 00.23"
Access & import/export	The specimen was collected under a Collaborative Agreement with the University of Antananarivo and various ministries (Ministry of Mines, Ministry of Higher Education) of the Madagascar government. Permits from the Ministry of Mines (Scientific Studies Authorization No 005/2010) and the Ministry of Higher Education/University of Antananarivo (No 76 PAB/10, Supporting documentation: - Scientific Authorization Studies No 007/2010, 005/2010, 006/2010, 009/2010) were used in support of field research were issued on 17 June 2010 and 18 June 2010, respectively.
Disturbance	This study involved minimal disturbance to the environment, as the fossil-bearing layer was within 0.70 meters of the surface in the locality.

Reporting for specific materials, systems and methods

We require information from authors about some types of materials, experimental systems and methods used in many studies. Here, indicate whether each material, system or method listed is relevant to your study. If you are not sure if a list item applies to your research, read the appropriate section before selecting a response.

Materials & experimental systems

n/a	Involved in the study	
☒	☐	Antibodies
☒	☐	Eukaryotic cell lines
☐	☒	Palaeontology and archaeology
☒	☐	Animals and other organisms
☒	☐	Human research participants
☒	☐	Clinical data
☒	☐	Dual use research of concern

Methods

n/a	Involved in the study	
☒	☐	ChIP-seq
☒	☐	Flow cytometry
☒	☐	MRI-based neuroimaging

Palaeontology and Archaeology

Specimen provenance

The holotype specimen (UA 10015) was recovered from locality MAD05-42 from the Upper Cretaceous Maevarano Formation, Mahajanga Basin, Madagascar. Permits from the Ministry of Mines (Scientific Studies Authorization No 005/2010) and the Ministry of Higher Education/University of Antananarivo (No 76 PAB/10, Supporting documentation: - Scientific Authorization Studies No 007/2010, 005/2010, 006/2010, 009/2010) were used in support of field research were issued on 17 June 2010 and 18 June 2010, respectively.

Specimen deposition

The holotype specimen of Falcatakely forsterae is reposited in the University of Antananarivo (UA), Madagascar with the collection number UA 10015 .

Dating methods

No new dates were obtained for this contribution; age constraint for the Maevarano Fm. is developed in Rogers et al. 2000.

☐ Tick this box to confirm that the raw and calibrated dates are available in the paper or in Supplementary Information.

Ethics oversight

Fossil collection and exportation were completed in compliance with permits issued by the Ministry of Mines (United Republic of Madagascar) and through a Collaborative Agreement with the University of Antananarivo and various ministries (Ministry of Mines, Ministry of Higher Education) of the Madagascar government.

Note that full information on the approval of the study protocol must also be provided in the manuscript.